Applied Catalysis B: Environmental 341 (2024) 123359

Contents lists available at ScienceDirect

Applied Catalysis B: Environmental

journal homepage: www.elsevier.com/locate/apcatb

Catalytic upgrading of a model polyethylene pyrolysis oil by hydroconversion over Ni-containing hierarchical Beta zeolites with tailored acidity

L. Briones [a,*], A. Cordero [a], M. Alonso-Doncel [b], D.P. Serrano [b], J.M. Escola [a,*]

[a] Group of Chemical and Environmental Engineering, Rey Juan Carlos University, c/ Tulipán s/n, Móstoles, Madrid 28933, Spain
[b] Thermochemical Processes Unit, IMDEA Energy Institute, Avda. Ramón de la Sagra, 3, Móstoles, Madrid 28935, Spain

ARTICLE INFO

Keywords:
Polyolefins
Hydroconversion
Ni/h-Beta
Dealumination
Oxalic acid

ABSTRACT

Valorization of waste polyolefins by a sequential combination of thermal pyrolysis and catalytic hydroconversion over a bifunctional metal/acid catalyst (e.g. zeolite) is an efficient route to produce transportation fuels. However, the zeolite strong acidity typically causes extensive cracking and loss of liquid fuels. In this work, mild dealumination with oxalic acid of a hierarchical Beta zeolite was used to achieve Ni 7%/h-Beta catalysts with Si/Al ratios within the 25 – 130 range. These catalysts were tested in the hydroconversion of a model mixture of LDPE thermal pyrolysis product (1-dodecene/n-dodecane, 50/50 w/w). The highest share of liquid fuels (~ 90%) was achieved over 7% Ni/h-Beta (SiAl = 130). Besides, due to its high accessibility and tailored acidity, the product contained a meaningful amount of isoparaffins (12%) and a negligible content of olefins (< 3.5%). Thus, this catalyst holds promise for plastic waste hydroconversion towards transportation fuels.

1. Introduction

The need for reducing landfilling rates [1] and the potential use of waste plastics as raw materials in different chemical processes has led to the development of several treatments for chemical transformation of plastics, especially polyolefins. Among them, fuels production seems to be especially relevant since liquid fuels are easy to store and to transport and have a high commercial value. Thus, high yields of gasoline and diesel fuels from low-density polyethylene (LDPE) [2,3], other polyolefins and their mixtures [4] may be obtained by a two-step process comprising thermal cracking of the polymer followed by catalytic hydroconversion of the obtained oils. The second step involves a number of catalytic transformations of the hydrocarbons mixture occurring under hydrogen atmosphere, such as the cleavage of the C-C bonds to produce short-chain hydrocarbons (cracking), the hydrogenation of C=C bonds, skeletal isomerization to produce isoparaffins, cyclization and aromatization. As a result, the so obtained products were practically deprived of olefins, showing enhanced shares of isoparaffins and moderate of aromatics, which increases their quality as kerosene and diesel transportation fuels [5,6].

Hydroconversion of the polyolefin pyrolysis oil requires a bifunctional catalyst, generally a metal with hydro/dehydrogenation ability supported on an acid porous solid (e.g. a zeolite) able to produce the carbocations that can undergo β-scission or skeletal rearrangement. On the other hand, due to the bulky feature of many of the products from polyolefin thermal cracking, there is a need of zeolitic catalysts showing a high accessibility to gain a better access to both metal and acid sites. In this respect, hierarchical zeolites are especially suitable as they are characterized by the presence of a bimodal pore size distribution comprising both the typical zeolitic micropores and the additional mesopores [7,8]. However, an important drawback of zeolites is their strong acidity that causes the occurrence of severe cracking reactions leading to the production of gases and, therefore, reducing the oil yield. In this way, ordered mesoporous materials (like Al-SBA-15 or Al-MCM-41) are known to induce less cracking but at the expense of very low isomerization and aromatization activities [2]. Thus, a proper combination of acidity and accessibility is required in order to maximize the yield of liquid fuels.

Ni is one of the most preferred hydrotreating metals due to its high hydro/dehydrogenation activity and low cost. The effect of the metal/acid balance in the physicochemical properties and final performance of bifunctional catalysts used in the hydrotreatment of oil fractions or hydrocarbons [9–12], plastics [13–15] or oily biomass [16–18] has been earlier reported in literature. Regarding to hydrocarbons and plastics,

* Corresponding authors.
E-mail addresses: laura.briones.gil@urjc.es (L. Briones), josemaria.escola.saez@urjc.es (J.M. Escola).

https://doi.org/10.1016/j.apcatb.2023.123359
Received 4 April 2023; Received in revised form 1 June 2023; Accepted 13 July 2023
Available online 5 October 2023

the main conclusions drawn were that a higher metal/acid ratio promotes olefins hydrogenation [10], increases hydroisomerization up to a certain level [14,19–22] and prevents secondary cracking by fast hydrogenation of the intermediates [23]. The metal/acid balance can be easily tuned by varying the amount of metal incorporated, generally by impregnation or ion-exchange, on the acid support. Alternatively, the metal/acid ratio can be varied by adjusting the amount of acid sites in the support modifying the Si/Al atomic ratios. Several options to get different Si/Al ratios can be envisaged [24]: direct modification of the chemical composition of the synthesis medium, desilication to decrease the Si/Al ratio or dealumination to increase it.

In the case of Beta zeolite, the aluminum content of the gel influences strongly the nucleation and growth kinetics, hence the final composition of the materials tends to be close to that which provides the maximum stability to the crystalline structure (Si/Al molar ratio = 10 – 30), especially in basic medium [25]. Dealumination with acid solutions is the classical alternative to increase the Si/Al ratio. It is generally combined with a previous steaming of the material which facilitates the extraction of framework Al, providing a better thermal stability and creating a secondary porosity [26]. Nevertheless, this extra porosity is usually made of isolated cavities and does not improve the diffusional properties of the material [27]. Numerous acid species have been employed to dealuminate Beta zeolites, such as HCl [28]; HNO_3 [29]; tartaric acid [30]; or ethylenediaminetetraacetic acid [31]. Interestingly, oxalic acid has resulted in very intense Al extraction from several zeolite structures [32,33]. This is caused by the dual function of this molecule, which acts as an acid, hydrolyzing the Al-O bonds, and as a complexing agent, forming aluminum trioxalate ($Al_2(C_2O_4)_3$), which is highly soluble at low pH. Zeolites with large, three-dimensional pores, such as Beta, and those with more surface defects, such as nanocrystalline ones, are easier to dealuminate [30,31]. The more aggressive the treatment, the higher the Al extraction [28–30,34,35]. However, excessively high acid concentrations or temperature may drive to Si-O bonds hydrolysis and the partial or complete loss of the crystalline structure [29].

In the current work we report the effect of a mild dealumination treatment with oxalic acid upon the crystallinity, textural and acidic properties of a hierarchical Beta zeolite synthesized by a protozeolitic units silanization procedure. These dealuminated hierarchical Beta samples were subsequently employed as supports of Ni to obtain bifunctional catalyst that were tested in the hydroconversion of a model LDPE thermal cracking oil consisting of a 1-dodecene/n-dodecane 50/50 w/w mixture. This approach has not been assessed before using as support high Si/Al hierarchichal Beta zeolite, which is a 3D large micropore zeolite with mesopores and medium-strong Brønsted acid sites and harnessing Ni as well, a less costly metal than the pricey noble metals Pt, Pd or Ru. On the other hand, other supports such as silica, alumina or amorphous silica-alumina were discarded because of their very low content of medium – strong Brønsted acid sites, that are required for hydroisomerization. Thus, the major goal of the study was to determine how the dealumination treatment affects the extent of the different reactions involved in the hydroconversion of the model mixture, affording the production of transportation fuels with upgraded composition.

2. Experimental procedure

2.1. Synthesis of the Ni/h-Beta catalysts

The parent hierarchical Beta zeolite sample was prepared by a protozeolitic units silanization method published elsewhere [36]. A solution containing aluminum (aluminum flakes, Aldrich, 99.9%) and silicon (fumed silica, Degussa) precursors, tetraethylammonium hydroxide (TEAOH, Alfa, 35% aqueous solution), as structure directing agent, and distilled water was aged at room temperature for 20 h. The molar composition of this gel was Al_2O_3: 60 SiO_2: 15.5 TEAOH: 1000 H_2O. The gel was then precrystallized in a 500 mL Teflon-lined autoclave reactor at 135 ºC for 3 days in order to obtain a suspension of the protozeolitic nanounits. Subsequently, 8 mol% (with regard to the silicon content) of the silanization agent, phenylaminopropyltrimethoxysilane ($(C_6H_5)NH(CH_2)_3Si(OCH_3)_3$, Aldrich, > 97%) was added to the suspension and left reacting under reflux at 90 ºC for 6 h. The organosilane was anchored to the surface hydroxyls forming an organic moiety that partially prevents the nanounits aggregation, thus avoiding the formation of large crystals. The suspension was finally crystallized in the autoclave reactor at 135 ºC for 7 days. The obtained solid products were recovered by centrifugation, rinsed with distilled water, dried overnight at 110 ºC and calcined in stagnant air at 550 ºC for 5 h. The final material (h-Beta) presents a bimodal micro/-mesoporous structure generated by the removal of the structure directing and silanization agents upon calcination.

The parent h-Beta sample was dealuminated by treatment with oxalic acid dihydrate solutions ($H_2C_2O_4{\cdot}2\ H_2O$, Scharlau, Reagent Grade) with varying concentrations (0.025, 0.05 and 0.5 M). For each experiment, 2 g of h-Beta were placed in a round-bottom flask and 100 mL of the acid solution were added. The flask was then placed in a thermostatic bath to keep the temperature constant during the experiment. The treated samples were recovered by vacuum filtration, extensively washed with distilled water, dried at 110 ºC overnight and calcined in static air at 550 ºC for 5 h to remove any trace of oxalic acid.

Nickel was incorporated as metallic phase on the zeolite samples by impregnation with a nickel nitrate hexahydrate (Aldrich, > 98.5%) aqueous solution using a solution volume to pore volume ratio of 2. The $Ni(NO_3)_2$ concentration was calculated to achieve 7 wt% metallic Ni in the final catalysts. This Ni content was chosen as the optimum one to maximize the yield of liquid fuels [14]. Impregnated samples were dried in a rotary evaporator at room temperature under vacuum for 6 h and then calcined at 550 ºC for 5 h with a heating rate of 20 ºC min^{-1} to decompose the nitrate group and leave nickel in the oxide form (NiO). The oxide was then reduced under 30 NmL min^{-1} hydrogen flow in a Micromeritics Microactivity Pro fixed bed reactor with a heating rate of 2 ºC min^{-1} up to 550 ºC.

2.2. Characterization of the zeolite Beta supports and catalysts

The crystallinity, Al content and Si species distribution of the parent and dealuminated h-Beta materials were determined by X-Ray diffraction (XRD), Inductively Coupled Plasma Atomic Emission Spectroscopy (ICP-AES) and ^{27}Al and ^{29}Si magic angle spinning nuclear magnetic resonance (MAS NMR), respectively. Ni-containing catalysts were characterized by XRD, hydrogen temperature-programmed reduction (H_2-TPR), transmission electron microscopy (TEM) and Ar adsorption-desorption isotherms at − 186.15 ºC.

X-Ray diffraction patterns were collected within the 5 – 50 º range in a "Empyrean" PANalytical® diffractometer using Cu-Kα radiation with a step size of 0.0263 º and a counting time of 957 s. From them, the crystallinity of the dealuminated samples was checked. Additionally, the average size of the NiO crystals in the calcined Ni-containing samples was obtaining by means of the Scherrer equation.

The Al and Ni contents were determined by ICP-AES on a VARIAN Vista AX Axial CCD Simultaneous spectrometer. The samples were digested in H_2SO_4 and HF prior to the analysis. Additionally, the concentrations of Brønsted and Lewis acid sites of the zeolitic supports were determined by in situ FTIR spectroscopy of pyridine adsorption. Prior to the analyses, the samples were pressed into ca. 10 mg cm^{-2} self-supporting wafers, degassed at 450 °C under high vacuum for 4 h and cooled down to room temperature. Pyridine adsorption (3.5 mbar) was performed at 150 °C for 20 min, and the desorption was controlled stepwise by evacuating the adsorption cell for 20 min at 150, 250, 350 and 450 °C, under high vacuum. The corresponding spectra were recorded with a Nicolet iS50 spectrometer equipped with MCT detector, employing 150 scans with 4 cm^{-1} resolution. The acid sites were

calculated according to the following bands (vibration mode of pyridine) and absorption coefficients: pyridinium PyH^+ band at 1545 cm^{-1} ($\varepsilon = 1.67$ cm mol^{-1}) and pyridine PyL band at 1455 cm^{-1} ($\varepsilon = 2.2$ cm mol^{-1}) [37].

The shares of tetrahedral and octahedral aluminum species were determined by the signals at − 54 and 0 ppm, respectively, in the ^{27}Al MAS NMR spectra obtained in a Varian Infinity Plus 400 instrument operating at 104.16 MHz with spinning rates of 12 kHz. Chemical shifts were referenced to $Al(H_2O)_6^{3+}$ as external standard. The formation of silanol groups by dealumination was followed by the evolution of the peaks at − 106 ppm (Q_3) and − 114 ppm (Q_4) in the ^{29}Si-MAS NMR spectra obtained at 79.4 MHz and using tetramethylsilane as standard.

The textural properties were determined from the Ar adsorption-desorption isotherms at − 186.15 ºC obtained in a Micromeritics 3Flex equipment. Prior to the analyses, the samples were outgassed at 300 ºC for 5 h. The BET equation was applied to determine the surface areas using the relative pressure range of 0.05 – 0.17 in the adsorption branch [38]. Total pores volumes were calculated at a relative pressure of 0.99. The external surface areas and micropore volumes were obtained using the t-plot method with the De Boer and Lippens equation to calculate the thickness (t) of the adsorbed monolayer [39]. The pore sizes distributions were determined by the non-local DFT method applied to the Ar adsorption-desorption isotherms at − 186.15 ºC considering a cylindrical pore configuration.

The reducibility of NiO was assessed by hydrogen temperature programmed reduction (H_2-TPR) tests in an AutoChem 2910 system. The analyses were performed under a 35 NmL min^{-1} flow of 10% H_2 in Ar and heating up to 800 ºC with a heating rate of 5 ºC min^{-1}. The size and location of the Ni particles were inferred from TEM images collected in a Philips TECNAI 20 microscope with a LaB_6 filament under an accelerating voltage of 200 kV. Previously the samples were dispersed in acetone in an ultrasonic bath and deposited on a carbon-coated copper grid.

2.3. Thermal cracking tests of LDPE

The thermal cracking reaction of pure LDPE (REPSOL) was performed in a stirred 100 mL stainless-steel autoclave reactor provided with gases inlet and outlet and heated by a ceramic oven. In the experiment, 30 g of the polyolefin was thermally cracked at 400ºC for 90 min under 1.5 bar of nitrogen. The obtained oil from the cracking was separated by distillation into hydrocarbon mixtures within the gasoline ($C_5 – C_{12}$) and diesel ($C_{13} – C_{40}$) fractions since no heavier products than C_{40} were detected. The analyses of both gasoline and gaseous fractions were done by gas chromatography in a Varian 3800 GC harnessing a 100 m length x 0.25 mm i.d. Chrompack capillary column. The gasoline fraction ($C_5 – C_{12}$) was also analyzed by the PIONA method in order to determine the respective contents of paraffins, isoparaffins, olefins, naftenes and aromatics. The diesel fraction was analysed in a Varian 3900 GC equipped with a 25 m length methyl silicone capillary column.

2.4. Catalytic hydroconversion tests

The catalysts were tested in the hydroconversion of a 50/50 wt% 1-dodecene (Aldrich, 95%) and n-dodecane (Aldrich, ≥ 99%) mixture. This is a model mixture representative of the composition of the LDPE thermal cracking oils, typically made up of similar amounts of n-paraffins and 1-olefins with a wide distribution of carbon atom numbers. In every reaction, 10 g of each compound were placed into the vessel of a stainless-steal autoclave reactor together with 0.4 g of the corresponding catalysts (catalyst to feed mass ratio = 1/50). The reactor is provided with gases inlet and outlet, ceramic oven, stirrer, and electronic controller. After sealing the reactor, inert atmosphere was ensured by passing nitrogen at 2 bar for 15 min and then hydrogen was cold-charged up to 20 bar. The temperature was set at 350 ºC with a heating rate of 10 ºC min^{-1} and the stirring speed was set to 500 rpm. After 45 min of reaction, the reactor was left cooling down to room temperature and then the gases were vented through an ice-cooled trap and collected in a gases bag. Liquid products were separated from the catalyst by vacuum filtration.

Gaseous and liquid products were analyzed by gas chromatography in a Varian GC-3800 apparatus equipped with a CP-7530 fused silica capillary column and a flame ionization detector (FID). The obtained chromatograms were evaluated with the Varian Star Detailed Hydrocarbon Analysis 5.0 software to determine the carbon atom number distributions and the PIONA (Paraffins, Iso-paraffins, Olefins, Naphthenes and Aromatics) composition of the products.

3. Results and discussion

3.1. Properties of the parent h-Beta and dealuminated samples

Aluminum was extracted from the h-Beta materials by leaching in an oxalic acid solution. Different samples were prepared by modifying the concentration of oxalic acid and they were named as h-Beta (X), wherein X stands for the actual Si/Al atomic ratio determined by ICP-AES analyses. The extraction of Al atoms from the zeolite framework may produce different effects: the modification of the acid properties of the material, the formation of an additional porosity, and the partial loss of the zeolite structure if the treatment is strong enough.

The first issue of interest is the dealumination level achieved with each treatment. Fig. 1 shows the correlation between the oxalic acid concentration and the final Si/Al ratio measured by ICP-AES. By increasing the concentration of oxalic acid, the initial Si/Al ratio of the h-Beta material (25) can be raised up to a maximum of 130 for the sample treated with 0.5 M oxalic acid, but the complete removal of aluminum atoms from the zeolite framework seems not to be possible under the tested conditions since the curve reaches an asymptotic value of 125 ± 6. Based on these results, four samples were further considered (the original h-Beta (25) and the dealuminated h-Beta (68), h-Beta (90) and h-Beta (130)), as representative of materials with different Al content.

The extraction of aluminum has direct effects on the acidic properties of the zeolitic materials. The concentration of Brønsted (BAS) and Lewis (LAS) acid sites, calculated from pyridine adsorption FTIR measurements, is shown in Table 1 and Fig. S1. For the dealuminated hierarchical Beta supports, both BAS and LAS diminished steadily with the extent of the Al removal by the oxalic acid treatment. Thus, the concentration of Brønsted acid sites determined at 150 ºC dropped from 0.148 in the pristine zeolite h-Beta (25) to 0.026 mmol g^{-1} for the most

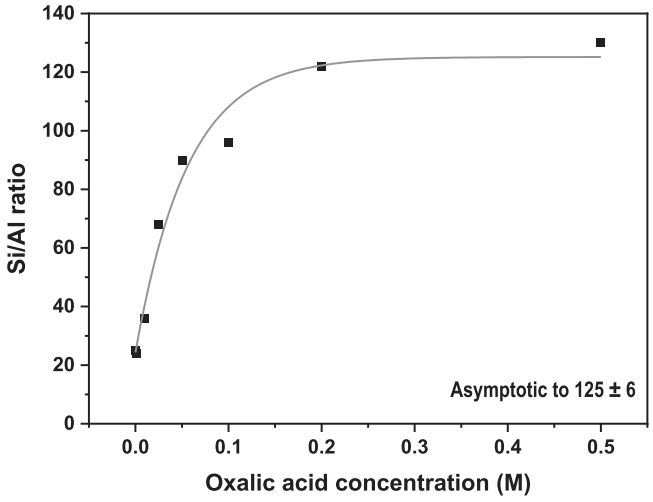

Fig. 1. Correlation between the oxalic acid concentration and the Si/Al atomic ratio of h-Beta samples.

Table 1
Physico-chemical properties of parent and dealuminated h-Beta samples.

Sample	Si/Al[a]	BAS (mmol g^{-1})[b]	LAS (mmol g^{-1})[b]	BAS/LAS	t-Al (%)[c]	o-Al (%)[c]	$\frac{Q3}{Q3+Q4}$[d]
h-Beta (25)	25	0.148	0.193	0.77	83.9	16.1	0.14
h-Beta (68)	68	0.065	0.105	0.62	90.7	9.3	0.21
h-Beta (90)	90	0.047	0.074	0.64	90.3	9.7	0.27
h-Beta (130)	130	0.026	0.077	0.34	87.5	12.5	0.30

[a] Measured by ICP-AES;
[b] Obtained by Pyr-FTIR at 150 ºC;
[c] Obtained from ^{27}Al MAS NMR spectra;
[d] Obtained from ^{29}Si MAS NMR spectra.

dealuminated h-Beta (130), while the respective amount of Lewis acid sites followed a variation from 0.193 to 0.077 mmol g^{-1}, respectively (Table 1). It is noteworthy that the concentrations of Lewis acid sites at 150 ºC was higher than those of the Brønsted acid sites for every zeolite sample but this trend change at higher temperatures for the dealuminated zeolitic supports. This is likely suggesting the occurrence of some extraframework aluminum species that have not been removed by the oxalic acid treatment and which are responsible of some residual weak Lewis acidity. Hence, the Brønsted acid sites did not fully disappear with the dealumination, being present even in the most dealuminated hierarchical Beta sample (SiAl = 130). This fact has certainly important catalytic implications since medium – strong Brønsted acid sites play a major role in both cracking and hydroisomerization reactions [40–42]. Moreover, the ratio between BAS and LAS tends to decrease with the intensity of the dealumination treatment, this effect being specially pronounced for the sample with the highest Si/Al ratio.

The shares of octahedral (o-Al) and tetrahedral (t-Al) aluminum species of the hierarchical Beta supports were calculated from ^{27}Al MAS NMR spectra [43], which can be found in Fig. S2. No other Al species, such as pentacoordinated aluminum, with signal around 30 ppm, were detected for any sample. The treatment with oxalic acid easily leaches extra-framework aluminum, lowering the share of o-Al from 16% corresponding to h-Beta (25) to 9% of h-Beta (68). Additionally, it is also able to remove framework Al, forming new o-Al species, so that the actual Si/Al ratios are reached. Therefore, both framework aluminum extraction and o-Al wash out occur simultaneously. This is in agreement with the dual function of the oxalic acid: hydrolyzing and chelating [32]. In overall, the share of o-Al species decreases initially with the intensity of the oxalic acid treatment but is enhanced again for the most dealuminated sample, which can be connected with the decrease in the BAS/LAS ratio observed for this sample. On the other hand, the treatment with oxalic acid has also a significant effect on the distribution of Si species, provoking the generation of new structural defects in the form of silanol groups. This fact is clearly observed by the increase of the $Q_3/(Q_3+Q_4)$ ratio, determined from the ^{29}Si MAS NMR spectra, in all the dealuminated samples regarding h-Beta sample, as it can be appreciated in Table 1. Thus, this ratio varies from 0.14 in the parent h-Beta sample to 0.30 for the material treated with the highest oxalic acid concentration.

Dealumination may also disturb the crystalline structure of the treated zeolites. The crystallinity of the Beta structure was checked by XRD (Fig. 2). All the materials present the typical diffraction patterns of the BEA structure corresponding to its both polymorphs A and B [44]. Notwithstanding, a certain loss in the intensity of the reflections can be observed for all the samples compared to the original h-Beta. This fact can be linked to the generation of structural defects upon

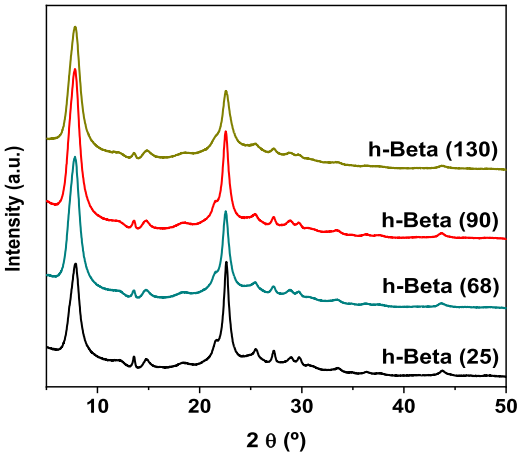

Fig. 2. XRD patterns of the original and dealuminated h-Beta zeolites.

dealumination. Minimal effects on the crystalline structure of several zeolites have also been described by previous authors after severe treatments [45]. On the other hand, a slight shift of the most intense reflection towards higher angles is detected for h-Beta (130), from 2θ = 22.4–22.6 °. This contraction of the lattice of Beta zeolites dealuminated with oxalic acid has been reported previously, being considered as a proof of the removal of t-Al atoms and formation of silanols [32].

3.2. Characterization of the Ni/h-Beta catalysts

The parent h-Beta and the selected dealuminated samples (h-Beta (68), h-Beta(90) and h-Beta (130)) were used to prepare bifunctional catalysts by Ni incorporation. The final Ni contents were similar for all the catalysts and close to the intended 7 wt%, ranging within 6.5 – 7.2%. The size and location of the metallic particles in the Ni-containing catalysts were determined by several techniques. Calcined materials – nickel as NiO – were subjected to XRD and H_2-TPR. After H_2 reduction – nickel as Ni^0 – the catalysts were characterized by TEM and Ar physisorption measurements at − 186.15 ºC.

Fig. 3 shows a selection of TEM micrographs of the Ni/h-Beta catalysts. The original h-Beta zeolite is made of small zeolitic nanounits around 5 – 10 nm size aggregated into particles of 200 – 400 nm. Despite dealumination, the general morphology of the supports does not change significantly: no amorphous material, disaggregation or pores formation were detected. For all the catalysts, a great part of the Ni particles are located on the external surface of the zeolite support, with some trend also to form aggregates.In this regard, Fig. S3 illustrates the Ni particle size distributions and the mean sizes obtained by direct measuring of more than 100 individual particles for each catalyst in a selection of TEM images. In every catalyst most of the Ni particles are within the 10 – 60 nm size, with slight differences between them. Ni/h-Beta (25) and Ni/h-Beta (130) present the largest particles – 37 nm average size –. On the other hand, the average Ni particle size obtained through the Scherrer equation applied to XRD patterns was rather similar, ranging within 26 – 36 nm.

The calcined catalysts were subjected to H_2-TPR (see Fig. S4). The obtained profiles were relatively similar for the dealuminated catalysts. NiO was always reduced in two stages centered at about 350 ºC and 430 ºC and reduction was complete at 550 ºC. The first stage (350 ºC) was ascribed to the reduction of large particles of bulk NiO while the second one (430 ºC) was associated to the occurrence of smaller nickel oxide particles interacting strongly with the support [46]. In contrast, NiO/h-Beta (25) presented a slightly different profile with only one major reduction stage centered at 430 ºC and a shoulder at 300 ºC, indicating that its higher Al content leads to a stronger metal-support

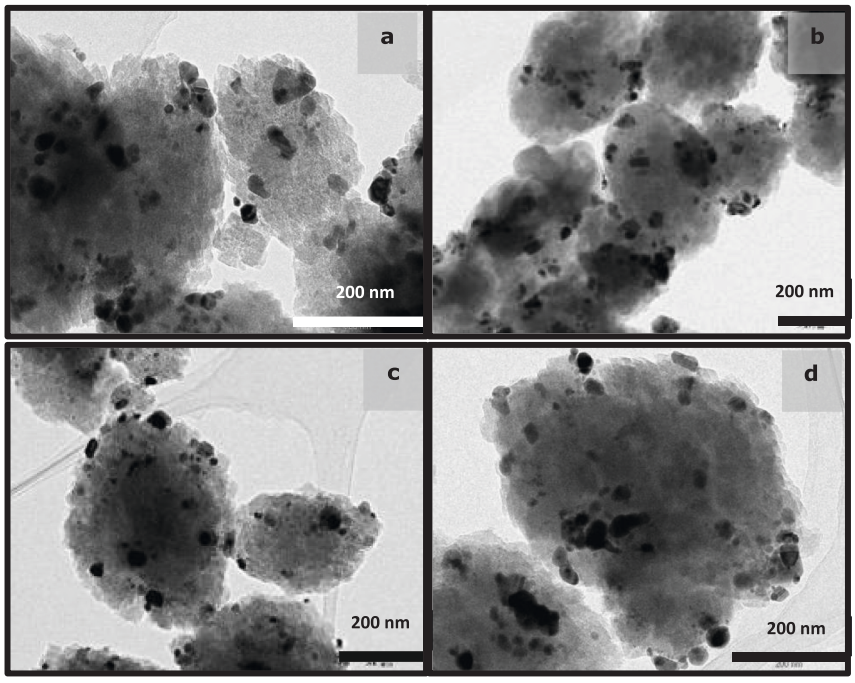

Fig. 3. TEM images of the different Ni-containing catalysts. (a) Ni/h-Beta (25); (b) Ni/h-Beta (68); (c) Ni/h-Beta (90); (d) Ni/h-Beta (130).

interaction.

The textural properties of the Ni-containing catalysts have been assessed by Argon physisorption at − 186.15 ºC. Thus, BET surface areas, total pore volumes at $P/P_0 = 0.99$, micropores volumes and external surface area values are summarized in Table 2. The shape of the isotherms in the dealuminated samples (Fig. S5) are close to that of the parent h-Beta (25), which may be regarded as a combination of type I and type IV isotherms according to IUPAC classification [47]. Thus, they exhibit an important Ar adsorption at low relative pressures ($p/p_0 < 0.001$) due to the filling of the micropores and a second important contribution in the 0.1 – 0.5 relative pressures interval corresponding to the capillary condensation into the hierarchical mesopores. Finally, a steeper slope is observed at higher relative pressures ($p/p_0 > 0.9$) that can be linked to condensation into inter-aggregates voids or macropores. In the particular case of the sample dealuminated with the highest oxalic acid concentration (Ni/h-Beta (130)), it presents an isotherm clearly below than that of h-Beta in the whole range of relative pressures. Fig. 4 depicts the cumulative pore volumes and the pore size distributions, determined by the NLDFT model. All the catalysts display a well-defined bimodal pore size distribution consisting of the typical zeolite micropores (around 0.6 nm) and the intraparticles mesopores (around 2 – 5 nm) generated by the protozeolitic seed silanization procedure [7].

Table 2 summarizes the textural properties of the Ni/h-Beta samples, showing some variations as a function of the dealumination treatment. An enhancement of both the BET surface area and the total pore volume is observed when using relatively small oxalic acid concentrations, which can be linked with the generation of structural defects with the dealumination process. However, this is not the case for the Ni/h-Beta (130) sample that exhibits distinctly lower values of the textural properties, suggesting that at high oxalic acid concentration some amorphous material could be formed due an excessive damage of the zeolite structure, being in agreement with the other changes above observed for this sample in terms of lower intensity of the XRD peaks and enhanced share of Lewis acid sites.

Table 2
Textural properties of the Ni/h-Beta catalysts.

Sample	S_{BET} (m^2 g^{-1})	V_T (cm^3 g^{-1})	V_{mic} (t-plot) (cm^3 g^{-1})	S_{ext} (t-plot) (m^2 g^{-1})
Ni/h-Beta (25)	510	0.386	0.189	115
Ni/h-Beta (68)	547	0.405	0.196	128
Ni/h-Beta (90)	523	0.434	0.201	109
Ni/h-Beta (130)	412	0.345	0.153	113

*Obtained from Ar adsorption-desorption isotherms at − 186.15 ºC.

3.3. Hydroconversion catalytic tests

The Ni/h-Beta samples prepared in this work are aimed to be used as catalysts in the hydroconversion of the pyrolysis oils derived from waste polyolefins pyrolysis for their upgrading towards transportation. In this way, Fig. 5.a illustrates the broad product distribution, in terms of atom carbon number, obtained in the low density polyethylene (LDPE) cracking at 400 ºC for 90 min under N_2 atmosphere. This product includes hydrocarbons within the C_2 – C_{30} range, with a majority of components corresponding to the gasoline and diesel fractions. Moreover, for each carbon atom number, the hydrocarbon mixture is made up mostly of similar amounts of the corresponding n-paraffin and 1-olefin. Likewise, Fig. 5.b shows the PIONA analysis of this LDPE pyrolysis oil that consists mainly of olefins (41 wt%) and n-paraffins (35%), and with distinctly lower amounts of isoparaffins (13%), naphthenes (5%) and aromatics (6%) as well. Accordingly, in this work, a model mixture of LDPE thermal cracking oil formed by n-dodecane / 1 – dodecene (50/50 w/w) has been chosen to assess the performance of the catalysts, based on the carbon atom number of Fig. 5, that is roughly centered around $C_{12,}$ as well as the previously shown PIONA analysis.

The four Ni-containing catalysts, selected and characterized in the previous section, have been tested in the hydroconversion of the n-dodecane / 1 – dodecene (50/50 w/w) mixture at 350 ºC for 45 min under 20 bar H_2 (initial pressure) with a mass catalyst to feed ratio of 1:50. Likewise, a blank test, without any catalyst, has also been performed in order to determine the extent of the bottom thermal reactions.

The classical theory of hydroisomerization over bifunctional catalysts indicates that the n-paraffin is hydrogenated/dehydrogenated over

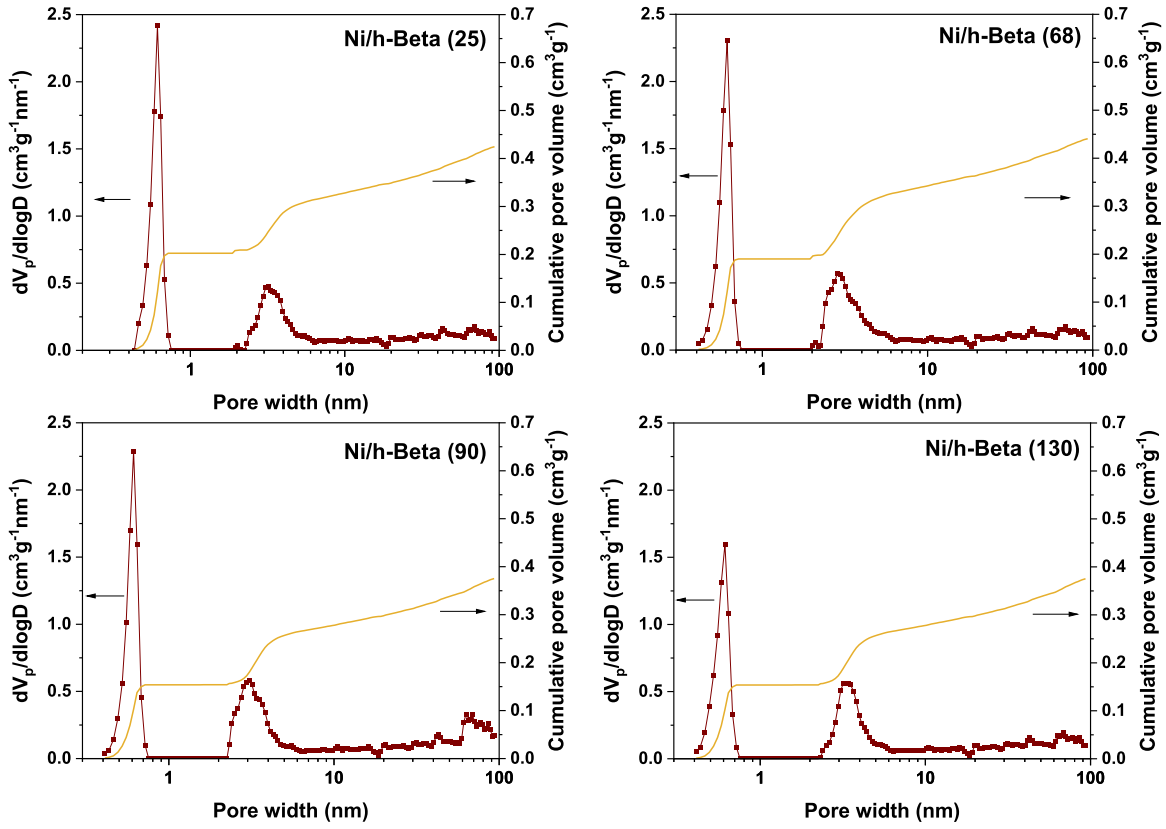

Fig. 4. Pores size distributions for the Ni/h-Beta catalysts obtained from the NL-DFT model applied to the adsorption branch of the Ar isotherms at – 186.15 ºC.

the metal site while over the Brønsted acid sites, the olefin is protonated originating a carbenium cation, that can undergo subsequently either skeletal isomerization or catalytic cracking mostly by β-scission [48–50]. In this respect, as one of the main goals of dealumination was to moderate the extent of cracking reactions leading to gases, the first point of interest is to check the evolution of cracking as the Si/Al atomic ratio is increased. Fig. 6.a presents the shares of gases C_1 – C_4 and other $< C_{12}$ hydrocarbons corresponding to the blank and catalytic tests. Although the gases fraction has been named as C_1 – C_4, no methane was detected for any reaction, ruling out the occurrence of hydrogenolysis. The blank test gives 8% of C_1 - C_{11} products, which are essentially C_1 – C_4, mainly ethylene and propylene. In contrast, hydroconversion over the parent Ni/h-Beta (25) leads to a very high yield of cracking products, almost 38%, being 21% of them gases, mainly C_4 (16.5%). It is noteworthy that the makeup of the $< C_{12}$ hydrocarbons shows an steady hike in the n-paraffins content on increasing the Si/Al atomic ratio of the catalyst, which is accompanied by a parallel abatement in the olefins amount (see Fig. 6.b). Thus, olefins contents dropped dramatically over any catalysts, below 12%. As hydrogenation of 1-dodecene was completed during the heating of the reaction medium, the final olefins were meant to be cracking and isomerization products, mainly 2-methyl-1-butene, 4-methyl-1-pentene and several C_7 olefins. On the other hand, as the Si/Al ratio of the zeolite rises by dealumination with oxalic acid, the number of Brønsted acids sites decreases and cracking drops, so for Ni/h-Beta (130) the share of $< C_{12}$ hydrocarbons abates to 22.6% (12% being gases). In this regard, the decrease in the amount of acid sites by augmenting the Si/Al atomic ratio is an effective way to diminish the extent of the cracking reactions. Thereby, the activity of the zeolites relies on the acid properties [51,52], and this explains the steady drop in the extent of the cracking reactions for the samples dealuminated at growing oxalic acid concentrations. However, despite the high Si/Al atomic ratio (130) of Ni/h-Beta (130) catalyst, its cracking activity is not negligible at all due to the presence of a significant BAS concentration still in this material. Regarding the distribution by atom carbon number of the cracking products (Fig. 6.c), it can be appreciated that C_4 compounds are the main components over all the catalysts, followed by C_5 hydrocarbons. Both components can be considered the primary products of end-chain cracking reactions. The yields of both C_4 and C_5 components decreases progressively with the intensity of the dealumination treatment, which is also an indication of the lower contribution of severe cracking reactions as the Al content of the h-Beta samples is lowered. On the other hand, a quite flat distribution is observed in the C_6 – C_{11} range, suggesting that these species are produced by random cracking reactions.

A second goal of hydrotreating is to hydrogenate the olefinic double bonds to prevent the appearance of unwanted products (i.e., gums formation in the injection systems of the automobiles). In this way, Fig. 7 shows the share of n-dodecane, 1-dodecene and other C_{12} compounds in the final products after reaction over each catalyst. A chromatographic analysis of the feed mixture indicated that its actual composition was 51% n-dodecane, 41% 1-dodecene and 8% impurities – mainly n-C_{11} and n-C_{13} –, which is close to the specifications of the providers. The blank reaction produced some gases formation, as stated above, and some oligomerization of light olefins into heavier hydrocarbons (4.8%) but no hydrogenation, since the final shares of n-dodecane and 1-dodecene were 47% and 40%, respectively. In contrast, in the catalytic reactions, all the tested catalysts were able to convert more than 98% of the starting 1-dodecene. This transformation is meant to happen in two stages: firstly, hydrogenation by the Ni particles to produce n-dodecane, since hydrogenation is the kinetically favored reaction that starts at lower temperatures (90 – 150 ºC). Secondly, at higher temperatures, the n-C_{12} is dehydrogenated over the Ni site and the resulting olefin undergoes cracking, isomerization, and cyclization chiefly at the Brønsted acid site according to the classical mechanism of paraffins conversion over bifunctional catalysts [14,48–50]. Thus, the less acidic catalysts lead to higher yields of n-dodecane. This agrees with the obtained results

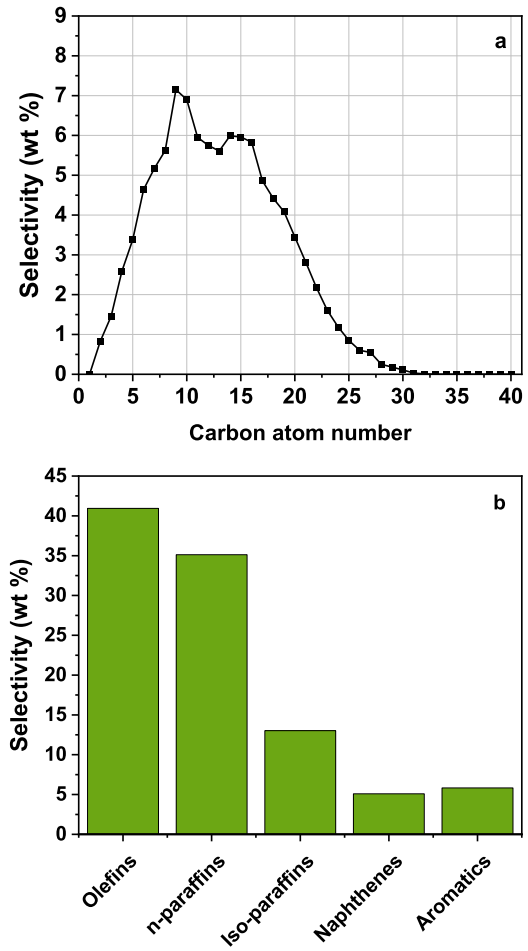

Fig. 5. Carbon atom number distribution (a) and PIONA analysis of the gasoline fraction (b) for a typical LDPE pyrolysis oil obtained at 400 ºC and 90 min in a batch reactor.

for the series of catalysts dealuminated with increasing oxalic acid concentrations: the yield of n-C_{12} increases from 50.6% for Ni/h-Beta (25) to 66.7% for Ni/h-Beta (130). Finally, all the catalysts provided a certain amount of products heavier than C_{12}, with yields ranging from 3.4% to 6.7%, due to oligomerization of light olefins. However, given that the blank test produced 4.8% $> C_{12}$ compounds, it seems that oligomerization is a mere effect of temperature.

The saturation of the olefins is necessary to increase the stability of the fuel and to prevent further oligomerization and gum formation. However, a too high content in normal paraffins is not desirable as it greatly lowers the RON of the gasolines and increases the pour point of diesel fuels. The distribution between normal and branched paraffins is the most relevant difference between products and is the key factor to determine the quality of the final fuels. The blank tests gave an iso-paraffins yield of 3.4% and the catalytic products raised this value up to 10 – 20%. This indicates that the ability of Ni/h-Beta to perform skeletal isomerization is preserved even for high Si/Al ratios. An increase in the oxalic acid concentration in the dealumination treatment led to a lesser isoparaffins formation, with yields ranging from 17.6% for Ni/h-Beta (25) to 11.7% for Ni/h-Beta (130).

Fig. 8 illustrates the weight ratio isoparaffins / n-paraffins versus the overall liquid fractions yield for the different Ni/h-Beta catalysts, showing that a trade-off is established between both parameters as the dealumination degree of the h-Beta is enhanced. In overall, lower acid sites concentration leads to higher yields of the liquid products but at the expense of less hydroisomerization activity. Thus, the iso-/n-paraffin ratio diminished from 0.26 (Ni/h-Beta (25)) to 0.15 (Ni/h-Beta (130)). As Ni/h-Beta (68) and Ni/h-Beta (90) present acid sites of similar nature (strength and tetra-/octahedral aluminum shares), seemingly the observed decrease in the number of Brønsted acid sites would explain the drop in isoparaffins / n-paraffins ratio for both samples. However, both Ni/h-Beta (90) and Ni/h-Beta (130) resulted in the same iso-paraffins / n-paraffins ratio. In this case, although the amount of Brønsted acid sites is lower over Ni/h-Beta (130), its higher Si/Al atomic ratio is likely to lead towards a greater separation between the metal and acid sites, which has been reported to increase the selectivity towards hydroisomerization over zeolites [53]. The balance between these two factors would account for the result over Ni/h-Beta (130). The occurrence of isoparaffins in the liquids is particularly important considering that they improve the cold flow properties of the fuels, such as pour point and freezing point, by decreasing their respective temperature values so they can be properly harnessed under cold weather seasons for transportation [54].

4. Conclusions

Treatment of a hierarchical Beta zeolite (SiAl = 25) with oxalic acid solutions of different concentrations has proved to be an effective dealumination treatment. However, complete removal of Al was not possible, and the maximum ratio achieved was 130 for the highest oxalic acid concentration (0.5 M). Framework Al extraction and subsequent wash out of the formed octahedral species occur simultaneously due to the dual hydrolyzing/chelating function of oxalic acid, keeping the tetrahedral/octahedral ratios approximately constant for all the dealuminated materials. Only at the highest oxalic acid concentration the crystalline structure of the zeolite seems to be somewhat affected. The content of BAS and LAS diminished steadily after the dealumination treatment but interestingly, the Brønsted acid sites did not disappear in any support, even in the most dealuminated sample, unveiling the occurrence of strong BAS as well. Characterization of the Ni-containing catalysts indicated that Ni particles were located in a great part on the external surface of the zeolite particles and their size was quite similar for all the catalysts. Additionally, the textural properties of the Ni/h-Beta catalysts were rather similar, except for Ni/h-Beta (130) catalyst, that showed lower values due to its inferior crystallinity. However, all the catalysts displayed the typical bimodal micropore/mesopore size distribution of hierarchical zeolites.

Hydroconversion activity of the zeolite samples was investigated using a model n-dodecane/1-dodecene mixture, which can be considered representative of the hydrocarbon types present in the thermal cracking oil of polyethylene. The catalytic hydroconversion results demonstrated that the dealumination degree achieved for the h-Beta zeolites affected significantly to both the activity and the product distribution. Initially, the decrease in the number of acid sites diminishes the extent of the cracking reactions, increasing the yields of useful liquid products. This abatement in the content of acid sites is accompanied by a reduction in the hydroisomerization ability, although the catalyst with the highest Si/Al atomic ratio (130) still holds a meaningful iso-parafffins production. Thus, the catalyst with the highest Si/Al atomic ratio (Ni/h-Beta (130), SiAl = 130) exhibited a remarkable performance, showing the lowest gases formation, moderate iso-paraffins production and the lowest olefins content. These results prove that the usage of Ni/dealuminated hierarchical Beta zeolite for the hydroconversion of the product of the thermal pyrolysis of polyolefin wastes holds promise to achieve higher yields of upgraded liquid fuels useful for transportation.

CRediT authorship contribution statement

L. Briones: Conceptualization, Investigation, Formal analysis, Data curation, Validation, Writing – original draft. **A. Cordero:** Investigation, Formal analysis, Visualization, Software. **M. Alonso-Doncel:** Investigation, Formal analysis, Resources, Validation, Data curation. **D. P.**

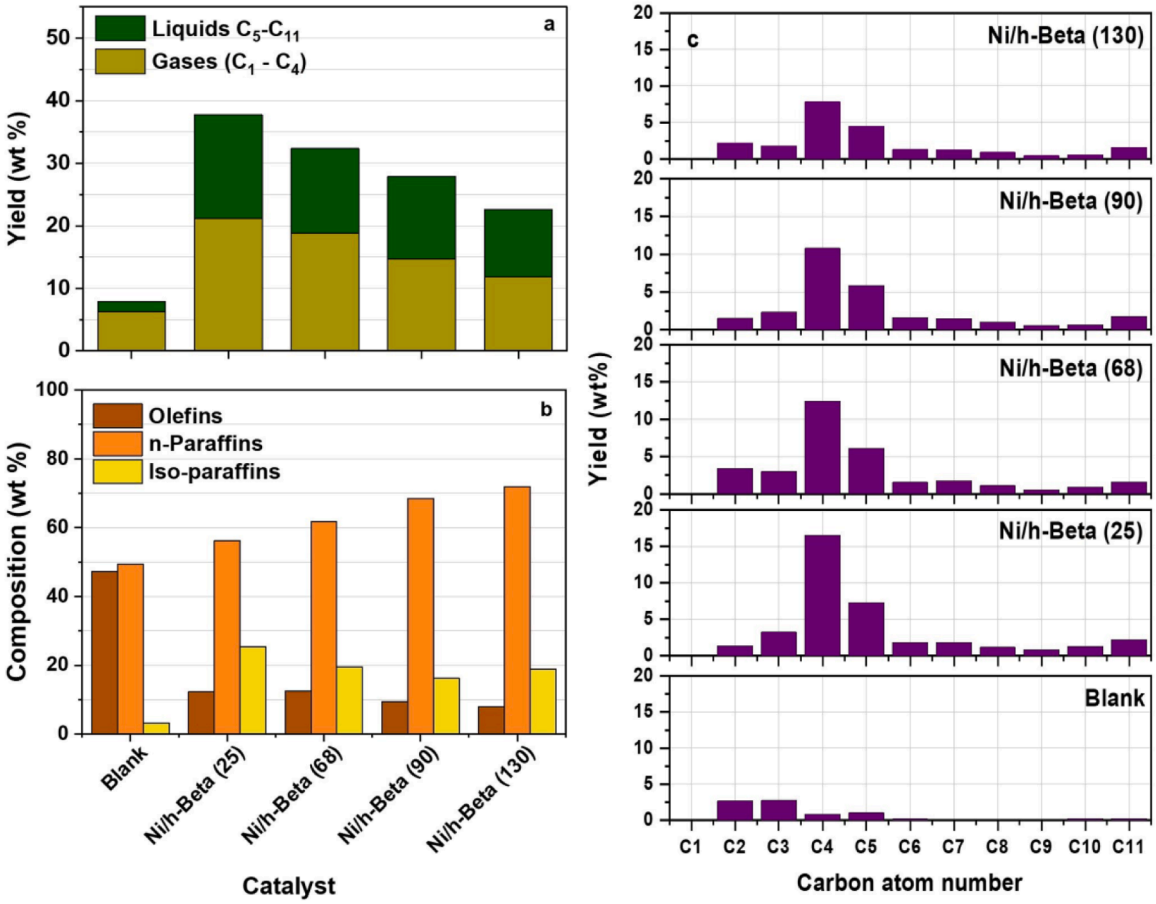

Fig. 6. Yield and composition of the $< C_{12}$ fraction in the hydroconversion of the model LDPE thermal cracking oil over h-Beta catalysts: (a) Yields to gases (C_1-C_4) and liquids (C_5-C_{11}); (b) PIONA composition of the gaseous + liquid products; (c) Product distribution by carbon atom number.

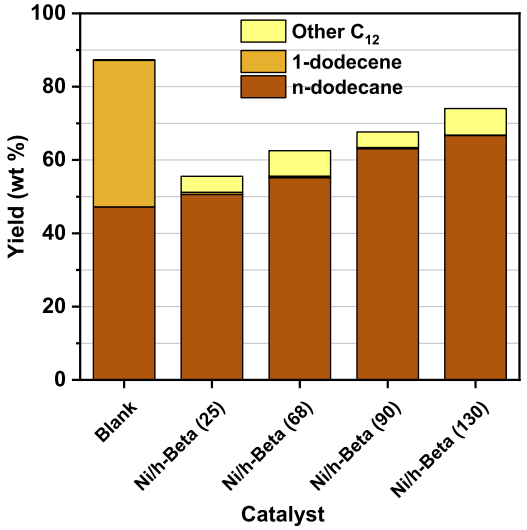

Fig. 7. Hydroconversion of the model LDPE thermal cracking oil over h-Beta catalysts: yields of the different C_{12} products.

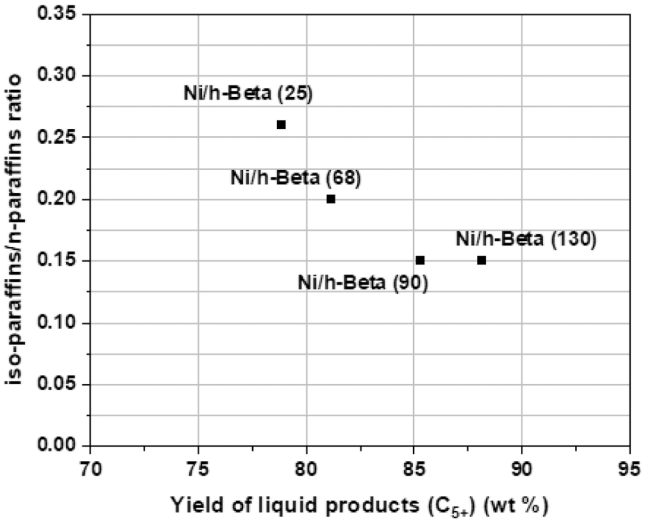

Fig. 8. Hydroconversion of the model LDPE thermal cracking oil over h-Beta catalysts: relationship between the Iso-/n-paraffins ratio and the overall yield of liquid products.

Serrano: Funding acquisition, Project administration, Supervision, Writing – review & editing. **J. M. Escola:** Conceptualization, Formal analysis, Supervision, Validation, Writing – review & editing.

Declaration of Competing Interest

The authors declare that they have no known competing financial interests or personal relationships that could have appeared to influence the work reported in this paper.

Data availability

Data will be made available on request.

Acknowledgements

The authors want to acknowledge the funding for this research by Spanish Ministry of Science and Innovation through project TRA2009–0111.

Appendix A. Supporting information

Supplementary data associated with this article can be found in the online version at doi:10.1016/j.apcatb.2023.123359.

References

[1] APME (Association of Plastic Manufacturers in Europe), 2014. Plastics – The Facts 2014 <⟨www.plasticseurope.com⟩>.
[2] J.M. Escola, J. Aguado, D.P. Serrano, A. García, A. Peral, L. Briones, R. Calvo, E. Fernández, Appl. Catal. B 106 (2011) 405–415.
[3] J.M. Escola, D.P. Serrano, J. Aguado, L. Briones, J.L. Díaz de Tuesta, R. Calvo, E. Fernández, Energy Fuels 26 (2012) 3187–3195.
[4] J.M. Escola, J. Aguado, D.P. Serrano, L. Briones, J. Mater. Cycl. Wast. Manag. 14 (2012) 286–293.
[5] V.L. Mangesh, T. Perumal, S. Subramanian, S. Padmanabhan, Energy Fuels 34 (7) (2020) 8824–8836.
[6] A. Bin Jumah, V. Anbumuthu, A.A. Tedstone, A.A. Garforth, Ind. Eng. Chem. Res. 58 (45) (2019) 20601–20609.
[7] D.P. Serrano, J.M. Escola, P. Pizarro, Chem. Soc. Rev. 42 (9) (2013) 4004–4035.
[8] D.P. Serrano, J. Aguado, J.M. Escola, Catalysis 23 (2011) 253–283.
[9] A. Lugstein, A. Jentys, H. Vinek, Appl. Catal. A 166 (1998) 29–38.
[10] J. Wang, Q. Li, J. Yao, Appl. Catal. A 184 (1999) 181–188.
[11] M.A. Arribas, P. Concepción, A. Martínez, Appl. Catal. A 267 (2004) 111–119.
[12] J. Francis, E. Guillon, N. Bats, C. Pichon, A. Corma, L.J. Simon, Appl. Catal. A 140 (2011) 409–410.
[13] W. Ding, J. Liang, L.L. Anderson, Energy Fuels 11 (1997) 1219–1224.
[14] J.M. Escola, J. Aguado, D.P. Serrano, L. Briones, Waste Manag. 34 (2014) 2176–2184.
[15] J.M. Escola, D.P. Serrano, J. Aguado, L. Briones, Ind. Eng. Chem. Res. 54 (2015) 6660–6668.
[16] S. Handjiani, E. Marceau, J. Blanchard, J.-M. Krafft, M. Che, P. Mäki-Arvela, N. Kumar, J. Wärnå, D.Y. Murzin, J. Catal. 282 (2011) 228–236.
[17] D. Kubička, J. Horáček, M. Setnička, R. Bulánek, A. Zukal, I. Kubičková, Appl. Catal. B 145 (2014) 101–107.
[18] C. Ochoa-Hernández, Y. Yang, P. Pizarro, V.A. de la Peña O'Shea, J.M. Coronado, D.P. Serrano, Catal. Today 210 (2013) 81–88.
[19] Y. Rezgui, M. Guemini, Appl. Catal. A 282 (2005) 45–53.
[20] A. de Lucas, P. Sánchez, F. Dorado, M.J. Ramos, J.L. Valverde, Appl. Catal. A 294 (2005) 215–225.
[21] C.M.N. Yoshioka, T. Garetto, D. Cardoso, Catal. Today 107–108 (2005) 693–698.
[22] A. Fúnez, A. de Lucas, P. Sánchez, M.J. Ramos, J.L. Valverde, Chem. Eng. J. 136 (2008) 267–275.
[23] G. Talebi, M. Sohrabi, S.J. Royaee, R.L. Keiski, M. Huuntanen, H. Imamverdizadeh, Ind. Eng. Chem. Res. 14 (2008) 614–621.
[24] H.K. Beyer, Mol. Sieves 3 (2002) 203–255.
[25] S. Mintova, V. Valtchev, T. Onfroy, C. Marichal, H. Knözinger, T. Bein, Microporous Mesoporous Mater. 90 (2006) 237–245.
[26] S. Bernasconi, J.A. van Bokhoven, F. Krumeich, G.D. Pirngruber, R. Prins, Microporous Mesoporous Mater. 66 (2003) 21–26.
[27] A.H. Janssen, A.J. Koster, K.P. de Jong, Angew. Chem. Int. Ed. 113 (2001) 1136–1138.
[28] M.M.L. Ribeiro Carrott, P.A. Russo, C. Carvalhal, P.J.M. Carrott, J.P. Marques, J. M. Lopes, I. Gener, M. Guisnet, F. Ramoa Ribeiro, Microporous Mesoporous Mater. 81 (2005) 259–267.
[29] R. Giudici, H.W. Kouwenhoven, R. Prins, Appl. Catal. A 203 (2000) 101–110.
[30] R. Srivastava, N. Iwasa, S. Fujita, M. Arai, Catal. Lett. 130 (2009) 655–663.
[31] A. Gola, B. Rebours, E. Milazzo, J. Lynch, E. Benazzi, S. Lacombe, L. Delevoye, C. Fernández, Microporous Mesoporous Mater. 40 (2000) 73–83.
[32] M.R. Apelian, A.S. Fung, G.J. Kennedy, T.F. Degnan, J. Phys. Chem. 100 (1996) 16577–16583.
[33] M. Müller, G. Harvey, R. Prins, Microporous Mesoporous Mater. 34 (2000) 135–147.
[34] J.C. Van der Waal, M.C. Rigguto, H. Van Bekkum, Chem. Comm. 10 (1994) 1241–1242.
[35] J.P. Marques, I. Gener, P. Ayrault, J.C. Bordado, J.M. Lopes, F.R. Ribeiro, M. Guisnet, Comptes Rendus Chim. 8 (2005) 399–410.
[36] J. Aguado, D.P. Serrano, J.M. Rodriguez, Microporous Mesoporous Mater. 115 (2008) 504–513.
[37] C.A. Emeis, J. Catal 141 (1993) 347–354.
[38] S. Brunauer, P.H. Emmett, E. Teller, J. Am. Chem. Soc. 60 (1938) 309–319.
[39] J.H. De Boer, B.C. Lippens, B.G. Linsen, J.C.P. Broekhoff, A. van den Heuvel, T. V. Osinga, J. Colloid Interface Sci. 21 (1966) 405–414.
[40] A. Peral, J.M. Escola, D.P. Serrano, J. Prech, C. Ochoa-Hernández, J. Cejka, Catal. Sci. Technol. 6 (2016) 2754–2765.
[41] J. Socci, A. Osatiashtiani, G. Kyriakou, T. Bridgwater, Appl. Catal. A 570 (2019) 218–227.
[42] G.E. Giannetto, G.R. Perot, M.R. Guisnet, Ind. Eng. Chem. Prod. Res. Dev. 25 (1986) 481–490.
[43] C.A. Fyfe, J.M. Thomas, J. Klinowski, G.C. Gobbi, Angew. Chem. Int. Ed. 22 (1983) 259–275.
[44] M.M.J. Treacy, J.M. Newsam, Nature 332 (1988) 249–251.
[45] C.S. Triantafillidis, A.G. Vlessidis, L. Nalbandian, N.P. Evmiridis, Microporous Mesoporous Mater. 47 (2001) 163–388.
[46] D.J. Lensveld, J.G. Mesu, A.J. Van Dillen, K.P. de Jong, Microporous Mesoporous Mater. 44–45 (2001) 401–407.
[47] M. Thommes, K. Kaneko, A.V. Neimark, J.P. Olivier, F. Rodriguez-Reinoso, J. Rouquerol, K.S.W. Sing, Pure Appl. Chem. 87 (9) (2015) 1051–1069.
[48] A. Corma, A. Martínez, V. Martínez-Soria, J.B. Montón, J. Catal. 153 (1995) 25–31.
[49] A. Fúnez, A. de Lucas, P. Sánchez, M.J. Ramos, J.L. Valverde, Chem. Eng. J. 136 (2008) 267–275.
[50] J.M. Moriewski, I. Morawski, Appl. Catal. A 283 (2005) 147–155.
[51] J.T. Miller, P.D. Hopkins, B.L. Meyers, G.J. Ray, R.T. Roginski, G.W. Zajac, N. H. Rosenbaum, J. Catal. 138 (1992) 115–128.
[52] P.V. Shertukde, W.K. Hall, J.-M. Dereppe, G. Marcelin, J. Catal. 139 (1993) 468–481.
[53] K. Cheng, L.C.J. Smulders, L.I. van der Wal, J. Oenema, J.D. Meeldijk, N.L. Visser, G. Sunley, T. Roberts, Z. Xu, E. Doskocil, H. Yoshida, Y. Zheng, J. Zečević, P.E. de Jongh, K.P. de Jong, Science 377 (2022) 204–208.
[54] H.W. Schablitzky, J. Lichtscheidl, K. Hutter, Ch Hafner, R. Rauch, H. Hofbauer, Biomass-.-. Convers. Biorefin. 1 (2011) 29–37.